Evaluation of Corrosion Resistant Alloys as Construction Material for Acidic Geothermal Wells

James Nogara[1]* and Sadiq J. Zarrouk[2]

[1] Energy Development Corporation (EDC), One Corporate Center, Ortigas Center, Pasig City, Philippines

[2] Department of Engineering Science, the University of Auckland, Private Bag 92019, Auckland, New Zealand

*nogara.jb@energy.com.ph

Keywords: *geothermal corrosion, acid fluid, corrosion resistant alloys, acid-sulfate chloride, casing, wellbore.*

ABSTRACT

A number of geothermal fields around the world have reported excessive corrosion in wellbore and wellhead appurtenances constructed from standard carbon steel material due to acidic fluids (Keserovic and Bäßler, 2013; K. Lichti et al., 2010; Mundhenk, et al., 2013; Sanada et al., 2000, Villa, et al., 2000; Abe, 1993; Amend and Yee, 2013). This work focuses on two types of acidic geothermal fluid: (1) acid chlorine + ($SO_4^{=}$) type and (2) acid sulfate + (chloride) type.

This report shows the damage to carbon steel piping material exposed to acid sulfate + (chloride) fluid with pH<3 from two geothermal wells in the Philippines. Surface analyses were performed on carbon steel pipes; electrical resistance (ER) probes and mass-loss coupon exposed to fluids from the two wells. The metal samples analyzed show excessive material loss and pitting. Corrosion rates measured exceed the allowable limit of 0.01 mm/y (Kurata, et al., 1995) for geothermal use. Corrosion products on the surface of the samples consist mostly of iron oxides and/or oxy-hydroxides indicating active transformation of metal to corrosion products. Silica and/or iron sulfides deposition were absent or negligible. Silica and iron sulfide deposits form a passive film inside the well and surface equipment which are normally a characteristics of less acidic alkali-chloride geothermal fluid.

A review of tests that have been conducted on different types of corrosion-resistant alloys (CRA) exposed to acidic geothermal fluid. These tests were done using either laboratory analogues or actual field corrosion tests on discharging wells. The performance of these alloys under corrosive conditions is reviewed with the goal of selecting materials for further field tests in an acidic (pH ~ 3) geothermal well in the Philippines.

Nine metals will be used for the test using standard mass-loss coupons mounted on pipeline test rack. The methods for evaluating the results of the field tests include:

- Uniform corrosion rate determination through mass-loss method
- Surface analyses using scanning electron microscopy (SEM).
- Characterization through energy dispersive x-ray spectroscopy (EDS) analyses.

The results will be used to recommend appropriate materials for further tests or field application.

1. INTRODUCTION

1.1 Corrosion in Geothermal Environment

Corrosion is 'the undesirable deterioration' or the adverse effects on the properties of a metal or alloy resulting from the interaction of the metal with its environment (Shreir, 1976). Corrosion occurs because processed materials such as metals and alloys have inherently high free energy that has a tendency towards more stable lower energy states such as corrosion products (Kain, 2012).

The corrosion behavior of geothermal fluid in the well and downstream pipelines, results from their chemical composition. This composition is related directly to the geological formations with which the fluids interact and percolate as they rise through the well (Casper and Pinchback, 1980). Corrosion behavior of geothermal fluid is enhanced by its high mineral content that imparts high electrical conductivity and favors the electrochemical corrosion process. Corrosion rates in water generally increase with temperature (Kritzer, 2004). High temperature also enhances corrosion characteristics of geothermal fluid by increasing the rates of chemical reactions and diffusion. Activity or concentration of H^+ (expressed as pH) plays a major role in metal corrosion specifically the corrosion of iron.

$$Fe + 2H^+ (aq) + 2\ Cl^- (aq) \rightarrow Fe^{2+} (aq) + 2\ Cl^- (aq) + H_2 (g) \quad (1)$$

Or simply:

$$Fe\ (metal) + 2H^+ (aq) \rightarrow Fe^{2+} (aq) + H_2 (g) \quad (2)$$

This can be further broken down into the half-cell reactions:

$$(Anodic) \quad Fe\ (metal) \rightarrow Fe^{2+} + 2e^- \quad (3)$$

$$(Cathodic) \quad 2H^+ + 2e^- \rightarrow H_2 (g) \quad (4)$$

At low pH, proton reduction takes place and the corrosion rate becomes higher as the pH decreases.

Other components of geothermal fluids that influence corrosion are (P. Ellis, 1985):

• Oxygen (generally from aeration)

• Sulfide species

• Carbon dioxide species

• Ammonia species

• Sulfate ion

This potential problem in handling corrosive geothermal fluids have been explored early on through corrosion tests carried-out in New Zealand (Marshall, and Braithwaite, 1973), USA (Banning and Oden, 1973), Iceland (Einarsson,

1960) and Mexico (Tolivia, 1970). From these tests, a number of materials were recommended for use in geothermal well construction and steam-field installations. The fluids tested were from neutral-pH moderately saline geothermal fluids. The results from these studies recommend the use of low – strength API standard casing for geothermal well casing strings and low strength low-carbon steels for cross-country pipelines for transmission of fluids from well head to power stations. Currently the NZ Code of Practice for Deep Geothermal Well (NZS 2403:1991) specifies the use of casing type and material conforming to API Spec 5CT or API Spec 5L standards. For API Spec 5CT, this includes types H40, J55, K55, M65, L80 type 1 and C90 type 1. For API Spec 5L, these are types A and B and X42 through to X65. Aluminum, brass and copper base alloys were found not suitable due to low corrosion resistance (Marshall and Hugill (1957). Wellhead equipment can be similarly constructed of low strength carbon steel but for valve trim, stainless steel should be used (Marshall, T., Braithwaite, W.R., 1973).

An early published guideline for geothermal construction materials can be found in Marshall and Braithwaite (1973). Miller (Miller, 1980) expounds further on materials selection for use in the Raft River Geothermal Experiment (RRGE) in Idaho, USA. This guideline includes not only metals but concrete and plastics materials recommended for geothermal application. A similar guideline was published by Radian Corporation entitled 'Materials Selection Guidelines for Geothermal Energy Utilization Systems' (Ellis and Conover, 1981). The guideline proposes a geothermal corrosivity classification with six classes based on developed geothermal fields at that time. The material recommendations do not depart significantly from those of Marshall and Braithwaite (1973) but expands on materials for use in geothermal heat pumps and heat exchangers.

As exploration of new geothermal fields continued, various types of geothermal fluids were encountered other than the neutral-pH moderately saline type. In the mid-70's, development of the Imperial Valley (USA) geothermal resources such as Salton Sea and Niland faced a new constraint in materials of construction. Hyper-saline and high temperature geothermal brine caused excessive corrosion rates to standard carbon steel.

A series of corrosion research have been conducted by the U.S. Bureau of Mines (Carter and McCawley, 1982; Cramer and Carter, 1980; McCawley, et al., 1981), Batelle - Pacific Northwest Laboratory (Shannon, et al., 1977) and Lawrence Livermore Laboratory (Harrar, et al., 1977; Harrar, et al., 1978; Harrar, et al., 1979). This work aimed to find suitable materials for use in brine and steam environments produced from high-salinity geothermal brines. Mass-loss and electrochemical corrosion measurements were conducted on over 60 metal alloys in brine and steam environments from 180 °C to 215° C, and in synthetic well Magmamax-1 brine at 105 °C and 232° C. General corrosion, crevice and pitting corrosion, and stress corrosion were examined along with the effects of dissolved gases. The alloys with the most acceptable corrosion performance in high-temperature, high-salinity geothermal environments were the high-chromium ferritic stainless steels, the Inconels and Hastelloys, and the titanium alloys (Cramer and Carter, 1980). Specific alloys that performed well in Salton Sea tests included Fe29Cr4Mo, E-Brite 26-1, stabilized Fe26CrlMo, 6X, Inconel625, Hastelloy C-276, Hastelloy S, Hastelloy G, Ti5OA, TiO.2Pd, and TiCode 12 (Cramer and Carter, 1980). Titanium Beta-C has proven to be highly resistant to corrosion in high-salinity brines and has shown to be more cost effective compared to other corrosion resistant casing (Holligan, et al., 1989; Schutz and Watkins, 1998).

Acid (pH) modification was also considered in the Salton Sea brine to control silica and mineral scaling. Because of this, a number of corrosion tests on acidified hyper-saline brine have been conducted (Goldberg and Owen, 1979; Posey and Palko, 1979; Shannon, 1977). Results show that in carbon steel corrosion increases as acidity increases. Corrosion rate increased 3-4 times with a 1 unit acidification (Shannon, 1977). It was observed from the tests that formation of corrosion product films or mineral scales can slow down corrosion. Corrosion products limit the transport of electrochemical species through the film.

Corrosion studies were also conducted in New Zealand to determine appropriate construction materials to handle geothermal fluids with high non-condensable gas (NCG) content such as in Broadlands-Ohaaki (Braithwaite and Lichti, 1980) and in hypothetical high gas geothermal fluids in the range of 25 ± 5% by weight (Lichti, and Julian, 2010). Their findings show that measured corrosion rates in separated water and separated steam were low and acceptable and comparable to those in fluids having more moderate gas concentrations. Carbon steel corrosion rate at two-phase flow condition was also low at 0.05 mm/y (Lichti and Julian, 2010).

The corrosive effects of acidic geothermal fluids have been recognized very early (Truesdell and Nakanishi, 2005). Geothermal wells are designed consciously to avoid acidic fluids. The formation alteration minerals from cuttings during drilling may be used as indicators of the presence of acid fluids (Reyes, 1985). The acceptable limit in terms of fluid pH for carbon steel has been normally set at 4.5. Below this pH corrosion rate is governed by hydrogen evolution rather than dissolved oxygen concentration (Baboian, 2005). Wells that produce highly acidic fluids (pH < 4.5) are plugged and usually abandoned. There are an estimated 38 drilled wells in Tiwi and MakBan geothermal fields that have been cement plugged due to acidity (Sugiaman, et al., 2004). Some geothermal fields have been abandoned all together due to acidity of produced fluid (Zarrouk, 2004). Examples of these are: Tatun geothermal field in Taiwan (Chen, 1970) and Alto Peak geothermal field in the Philippines (Reyes, et al., 1993).

Sanada, et al (2000) proposed a materials selection guideline that incorporates for acidic geothermal fluid down to pH > 2. The guideline also includes corrosion inhibition and pH modification aspects of corrosion control. No alloy material is recommended for use below pH 2.

Finding suitable materials for handling acid geothermal fluids offers substantial economic incentive. Some very productive geothermal wells drilled lately in Sibayak and Lahendong in Indonesia (Keserovic and Bäßler, 2013) and recently in well IDDP1 in Iceland (Ármannsson et al., 2014) has been producing highly corrosive acid fluids.

1.2 Acidic Geothermal Fluids

Sanada et al (1997) summarized the published chemistry data from acid wells from Japan, Philippines and Salton Sea, USA. Other published acid fluid chemistries are available in Einarsson, et al, 2010; Marini et al., 2003, Gherardi, et al., 2005; Abe, 1993; Mundhenk, et al., 2012, Koestono, 2010; Armansson, et al., 2014; and Truesdell, 1991). Three types of acid fluid were identified from geothermal well

discharges that have caused damage to geothermal wells and pipelines: **(1) acid CI-SO_4 waters with excess chloride, (2) HCl in superheated steam,** and **(3) acid SO_4-CI reservoir waters**.

One of the earliest published reports on a geothermal well with acid Cl-SO_4 waters with excess chloride discharge was in April 1960, in Senkyoro well No. 6 in Japan. Noguchi, et al., (1970) postulated that a small amount of ground water has mixed with a large amount of volcanic gases rising from deep. This reaction produced a liquid with high concentration of corrosive hydrochloric acid underground. Sulfuric acid in the discharge is believed to form from sulfur compound in volcanic gases through oxidation with air. All metals such as iron, aluminum, calcium, magnesium, sodium, manganese, uranium and thorium in the geothermal water are postulated to be derived from the surrounding rocks by the corrosive action of sulfuric acid. Other fields that have reported this type of acidity include Tatun geothermal field (Chen, 1970; White and Truesdell, 1969; Zarrouk, 2004), and in Krafla (Einarrson et al, 2010).

Hydrochloric (HCl) acid in super-heated steam has been reported in the Geyser's (Truesdell, et al., 1989), Los Humeros (Tello, et al, 2000) and Larderello (D'Amore and Bolognesi, 1994a). Hydrochloric acid (HCl) is transported only in superheated steam because below 300°C it is very soluble in neutral liquid and would have been removed from the vapor if condensate were present. The origin of the HCI in steam dominated fields is related to high-temperature reactions, which mainly forms from boiling of near-neutral NaCl brines or from reaction of halite with silicates (D'Amore and Bolognesi, 1994b). At The Geysers and Larderello, HCl in steam is closely related to the existence of high-temperature zones below the main vapor-dominated reservoir (Walters et al., 1988; D'Amore et al., 1990). In most areas of The Geysers where HCl occurs, steam is sufficiently superheated that the first condensation occurs at the wellhead and corrosion can be prevented by injection of alkaline solutions (e.g. caustic soda). Casings and surface piping of wells with high-CI steam have shown accelerated corrosion and in some cases experiencing failure (Hirtz, et al., 1991)

Acid SO_4-Cl reservoir fluids are common in arc-type geothermal systems along the circum-Pacific rim (Pang, 2005). Low pH well discharges in the geothermal systems of Japan and the Philippines are more enriched in oxygen-18 or deuterium or both as compared to neutral pH waters found in the same systems such as in Sumikawa, Japan (Ueda, et al., 1991) and Mahanagdong, Philippines (Salonga, et al., 2000) Isotope enrichment of both oxygen-18 and deuterium means higher percentage of magmatic vapor contribution to the well discharges due to the fact that un-neutralized magmatic water carries much abundant hydrogen ions to keep the water at a lower pH (Pang, 2006).

Deep acid-sulfate fluids have been encountered in many volcanic geothermal systems, particularly in association with andesitic volcanoes ((A. H. Truesdell et al., 1989); (Arnórsson, Stefánsson, & Bjarnason, 2007; Salonga, Bayon, & Martinez, 2000) and (Matsuda, Shimada, & Kiyota, 2005) . The sulfur species in acid sulfate-chloride thermal water are shown to be volcanic exhalations (Kiyosu and Kurahashi, 1983). The acidity is caused by HCl or HSO_4^- or both, and evidence indicates that it mostly forms by transfer of HCl and SO_2 from the magmatic heat source into the circulating fluid. When measured at 25 °C, the pH of flashed acid-sulphate water collected at the wellhead may be as low as 2. However, the pH of the water is near neutral at the high temperature in the aquifer. Production of acidity upon cooling is related to the increased acid strength of HSO_4^- with decreasing temperature (Villa, et al., 2000). The sulphuric acid type fluid is generally formed by any of three kinds of mechanisms, (1) oxidation of H_2S, (2) hydrolysis of SO_2, or (3) hydrolysis of S (native sulphur) (Matsuda, et al., 2005). The most important difference between the Na-Cl and acid-sulphate waters is that the main pH-buffer of the former is CO_2/HCO_3^-, but HSO_4^-/SO_4^{-2} in the latter. Compared to Na-Cl waters, acid SO_4-Cl waters contain higher concentrations of $SO_4^=$ and some minor elements, such as Fe and Mg, which are contained in minerals with pH-dependent solubility (Arnorsson and Stefansson, 2007).

2. DAMAGE TO CARBON STEEL BY ACID GEOTHERMAL FLUID

Carbon steel components exposed to geothermal wells discharging acid SO_4-Cl type fluids were surface analyzed. A Scanning Electron Microscope (SEM) coupled to an Energy Dispersive X-Ray Spectroscopy (EDS) was used for analyses. Table 1 details the physical and chemical parameters of the fluid environment were the samples were subjected to. The pH of the fluid from the two wells is less than 3. Higher concentration of SO_4 is observed in well X6D compared to well X2D but fluid from well X2D is more saline. Both wells are high-temperature with downhole fluid temperature approaching 300°C. The samples were exposed to the fluid at varying duration, the longest being the stinger pipe which was exposed for 43 days. No temperature measurements were made at exposure conditions. However, this can be referenced as saturated steam temperature at the indicated line pressure. The temperature condition in samples exposed to well X2D fluid is about 173°C, while for X6D samples it is estimated at 185°C except for the low pressure samples which is estimated at 140°C. Note that the fluid pH was measured at laboratory condition at around 25°C.

The cylindrical probes A and C (Figures 1 and 3) were the sensing element of an electrical resistance (ER) monitoring system used to measure the on-line corrosion rates of carbon steel pipeline from the two acidic wells. Sample B in Figure 2 is a section of a 1" by-pass line attached to the branch line of well X2D were acidic fluid was flowing continuously for about 1 month. Metal sample D in Figure 4 is a small piece of a 4"-diameter stinger installed inside well X6D to stabilize a capillary tubing inserted inside the well. Damage to the stinger was extensive with more than 50% material loss due to uniform corrosion and formation of deep cavities and pits throughout the metal surface. A small wedge shaped piece (about 1 cm) of the sample was cut near the pipe thread to examine the corrosion products inside the pipe (Figure 7).

Sample E in Figure 5 shows a commercial A106 grade B carbon steel metal coupon that was used to measure corrosion rate in well X6D through mass-loss method. The coupon was inserted into the two-phase line of well X6D using a retractable coupon holder. Note that large pits developed around the surface of the coupon and the edge of the coupon opposite the fluid flow direction was visibly eroded. Crevice corrosion is also evident along a circular outline where the retractable coupon holder washer made of polyethylene was previously attached.

Table 1 Physical and chemical data of the fluid environment where the samples were exposed. Although no definite exposure period is indicated for ER probe in well X2D, the estimate is less than 1 week.

	LABEL	pH	Pressure Mpa (g)	Chloride mg/kg	SO_4 mg/kg	Exposure Days
Well X2D						
Electrical Resistance cylindrical probe	**A**	2.56	0.76	10086	957	nd
carbon steel pipe material	**B**	2.56	0.76	10086	957	31
Well X6D						
Electrical Resistance cylindrical probe	**C**	2.47	0.28	3947	3187	10
carbon steel pipe material	**D**	2.47	1.02	3947	3187	43
Flat strip coupon	**E**	2.47	1.02	3947	3187	14

The ER probes (Figures 1 and 3) were cut across the diameter and set in resin and polished. From the cut section (Figure 6), the inner materials such as the wiring and the ceramic filling are clearly visible. The un-corroded metal can be observed in contrast to corrosion products deposited around the outside surface of the probe body. This transition area is examined at low and high magnification in the SEM (Figures 8 and 11). The wedge-shaped section that was cut from the 1"-pipe has a layer of (about 1 mm thick) corrosion products uniformly lining the inner wall. The scanning electron micrographs of the scales deposited are shown in Figure 9. Micrographs of chipped corrosion product from sample D is shown in Figure 10. Surface micrographs of the A106-B grade carbon steel coupon are shown in Figure 12.

Analyses of the composition in weight percent of the materials on the surface of the samples are shown in Table 2. Elements that can be identified using EDS are only those that have atomic weights heavier than beryllium. As such, hydrogen, helium and lithium are not included in the quantification (Shindo and Oikawa, 2002).

Corrosion product in the samples exposed to X2D fluid that consists (in terms of weight percent) mainly of iron and oxygen with traces of sulphur, silica, and chloride. The absence of significant amounts of silica in the scales indicate the scale is mostly a product of the transformation of the carbon steel material to iron oxides or oxy-hydroxides instead of being re-crystallized from the geothermal fluid. This is in contrast to the observations of Braithwaite and Lichti (1980) and Borshevska et al (1980) of the formation of magnetite layer overlain by an iron-sulfide (pyrite – pyrhottite) matrix observed in Broadlands-Ohaaki fluid. Goldberg and Owen, (1979) noted in their study of corrosion products in geothermal fluid that Fe and Si composition in the scales formed varied from 21% – 57% and 0.6% to 6.7% respectively. This fluctuation in Fe and Si composition was interpreted to be the replacement of Fe in the original corrosion product by Si from the scale. This is thought to be a transition zone between scale and corrosion product.

Note that in the tests conducted by Shoesmith, et al. (1980) on aqueous H_2S fluids. The dominant process observed at pH 2.7 is the direct dissolution of iron and only small traces of cubic ferrous sulphide and small traces of mackinawite developed on the metal surface. The appearance of the X2D samples in this case may be similar.

Iron and oxygen also dominate the composition of the scale in the samples exposed to well X6D. No traces of sulfur, or silica were detected from the samples. However, carbon is found in significant quantity. This may lead to the conclusion that iron-carbonates (as $FeCO_3$) may be present in the sample along with the iron oxides. However, $FeCO_3$ is known to develop typically at higher pH (pH>6) and can re-dissolve when the solution becomes more acidic (Fajardo, et al., 2013).

The composition of the scales in the A106 B corrosion coupon (Table 2) is more distinct than the rest of the samples analysed. The composition of the scale is more varied and includes large amount of zinc and arsenic. These elements are not significant components of A106B type carbon steel and may come from re-crystallized minerals deposited along with the iron oxide. Note that the abundance of silica in the scale may act as a deposition (nucleation) surface for other minerals from the fluid itself. This may explain why other elements are observed in this sample compared to the rest of the samples. As to why there is abundant silica in the scale matrix is not clear at this time.

Figure 1 Carbon steel cylindrical electrical resistance (ER) probe exposed to well X2D fluid. This probe was cut along the diameter and mounted on resin (Figure 6) to view the corrosion behavior on the metal surface.

Figure 2 Carbon steel pipe (1") used to transmit X2D fluid for 1 month at low flow condition. A section of pipe was cut near the thread (Figure 7). The inner surface of the pipe is coated with corrosion product and scale.

Deep pits are observed to form around the outer surface of the ER probe (Figures 8 and 11) as well as a general transformation of the metal into corrosion products. The corrosion product appears to be tightly adhering to the surface of the metal due to the absence of space in between

them, but the corrosion product is fragile and shows cracks at certain points from where acid fluid can penetrate and react with the metal thereby resulting in continuous material loss. The corrosion rate of carbon steel in well X2D

Figure 3 The sample above is the remaining piece of a cylindrical ER probe used to monitor well X6D corrosion rate. After 10 days of exposure half of the probe was cut due to corrosion.

Figure 4 A piece of 4" diameter carbon steel pipe used as a capillary tubing stinger inserted into well X6D. More than half of the stinger has been lost due to corrosion before it was retrieved.

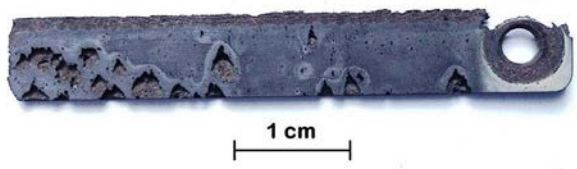

Figure 5 Carbon steel (A106-B Grade) mass loss coupon (flat strip) exposed to well X6D fluid for 14 days. The coupon was inserted inside the two phase pipeline of the well using a retractable coupon holder. Note the large corrosion pits on the surface of the coupon. The coupon edge facing the downstream flow of the fluid is eroded.

measured from this probe is 9.3 mm/y. This is higher as expected compared to the corrosion rate of 3.3 mm/y measured by Miranda-Herrera, et al. (2010) for ASTM A53 Grade B carbon steel exposed to geothermal fluids in Cerro Prieto with pH about 4.5. This is because the fluid in well X2D is more acidic and exposure is at a higher temperature. Shannon, et al (1977) observed than corrosion rates increase 3 – 4 times with 1 unit decrease in pH.

When viewed at 20,000X magnification, the corrosion products appear as fibre-shaped crystals (Figure 11) possibly iron oxy-hydroxides (FeOOH). Well-formed hexagonal disc-shaped crystals are found on the inner surface of the 1" pipe. The scale is untouched prior to the analyses being inside the pipe walls which prevented damage to the crystal from rubbing and handling. Further work using x-ray diffractometry (XRD) is needed to determine the exact identity of individual crystals in the scale deposits.

Even at low magnifications, samples C, D and E show extensive damage (Figures 10 -12). The metal has been completely transformed to brittle corrosion products that are easily abraded. There is general corrosion observed throughout the surface of the metal as well as deep pits observed in the ER probes (Figure 11). At high magnification, several crystal types are observed in the scale possibly indicating different minerals including iron carbonates in addition to iron oxides. The crystals in sample E (Figure 12) have been damaged due to handling but appear to be similar in sample D (Figure 11). The corrosion rate measured from this coupon is 0.68 mm/y.

Figure 6 Cylindrical ER probe cut across the diameter and mounted on resin and polished. Note the wire and ceramic inside the probe. Scale and corrosion products line the outer wall of the probe.

Further work is needed to identify the corrosion products beyond chemical composition provided by EDS. Borshevska, et al. (1982) used an x-ray diffractometer to

Figure 7 A small section (about 1 cm long) was cut from the pipe in Figure 2 and attached to a stub mount. The inside surface of the pipe is covered with about 1 mm thick corrosion product.

study the crystal patterns of corrosion products and identify individual minerals in the corrosion products. Another method would be to use a Transmission Electron microscope (TEM) in in conjunction with XRD similar to the approach of (Harrar et al., 1979).

Handling of the samples from field exposure to the laboratory presents a constraint in preserving the crystals developed during fluid exposure of the samples. Fluid trapped in the mineral scale tends to react with the scale over time at much lower temperature than in the original test environment. These samples have been in storage for a number of weeks and are vulnerable to this problem. In subsequent work, surface analyses should be done as soon as the samples are retrieved from the test facilities.

3. CORROSION TESTS USINGS CRA'S IN ACIDIC GEOTHERMAL WELLS

A database of various metals and corrosion resistant alloys that have been tested in acidic geothermal fluids or laboratory fluid analogues have been created as part of this study. A total of 87 distinct metals and alloys have been tested in geothermal fluid based on published information. Data were collected from 30 research reports and papers dealing with corrosion tests of metals and alloys in geothermal fluids. The database contains the following

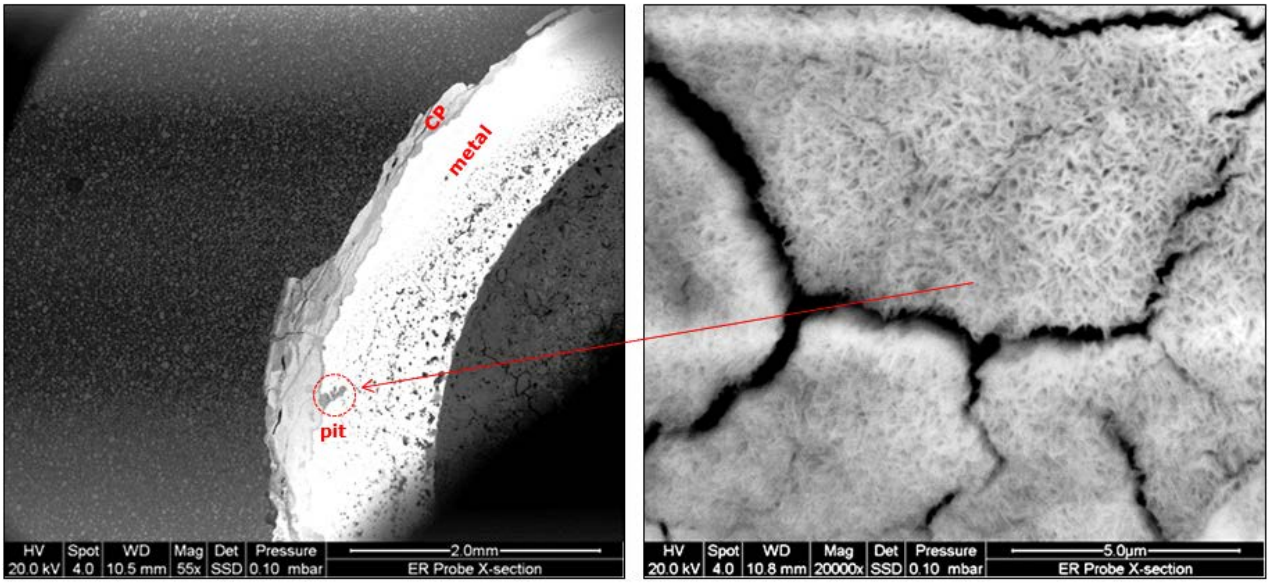

Figure 8 Scanning electron micrograph of the cylindrical ER probe cross-section. Low magnification image (left) show the metal and corrosion product (CP) interface. General corrosion is evident around the metal surface with occasional deep pits. High magnifications image of the pit area (right) shows the texture of the iron-oxygen corrosion product. Cracks developed within the CP matrix allowing the fluid to penetrate deep into the metal surface and continue the corrosion process.

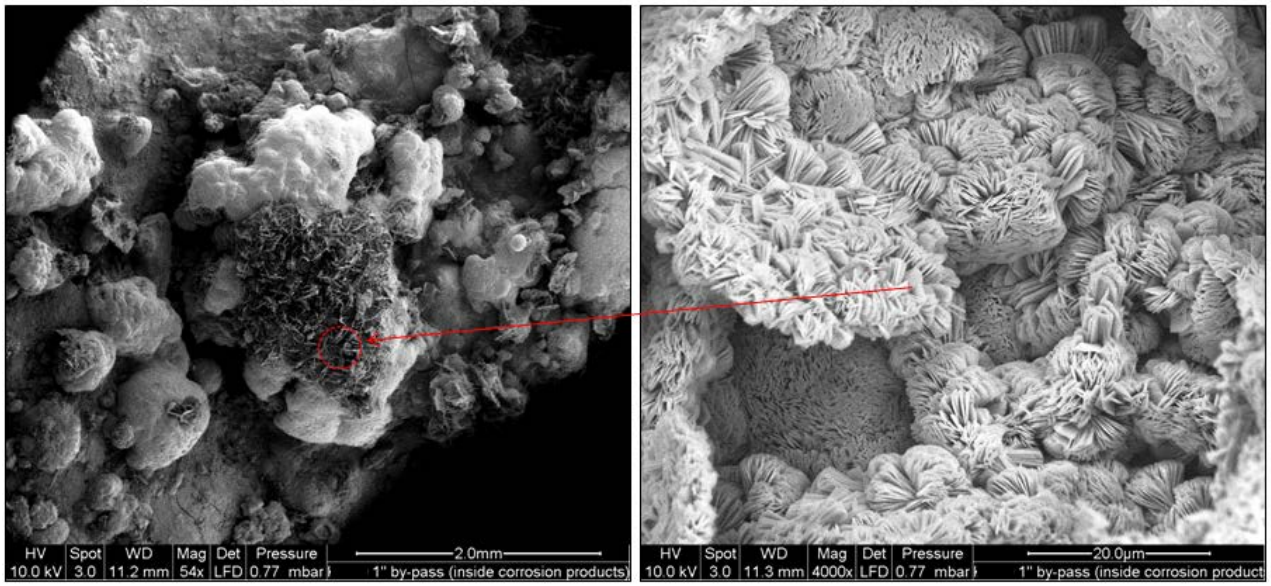

Figure 9 Corrosion product deposited inside the 1" carbon steel pipe used in well X2D. Right shows high magnification image of the iron-oxygen corrosion product with hexagonal plate crystal structure.

information pH, temperature, chloride concentration and fluid velocity as these were almost always indicated for each test. Although, hydrogen sulfide, sulfate and oxygen concentrations are important from a corrosion standpoint, most of the tests did not specify these parameters.

Although attempts have been made to identify each metal or alloy using the Unified Numbering System (UNS), most authors did not provide this information. Usually the researchers indicate the common or commercial names for the metal or alloy tested with a few exceptions. The UNS number is not a specification, because it does not provide the

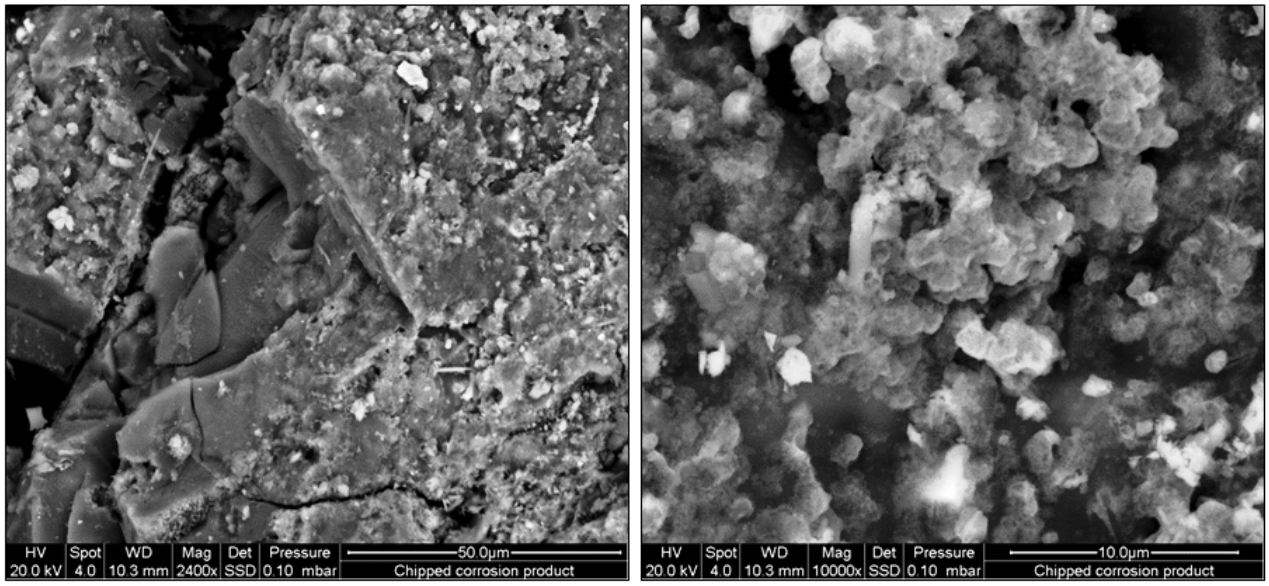

Figure 10 Chipped corrosion products from the carbon steel pipe exposed to well X6D fluid. The metal has been completely transformed to brittle corrosion product without any clear crystal pattern (amorphous?) shown at high magnification (right).

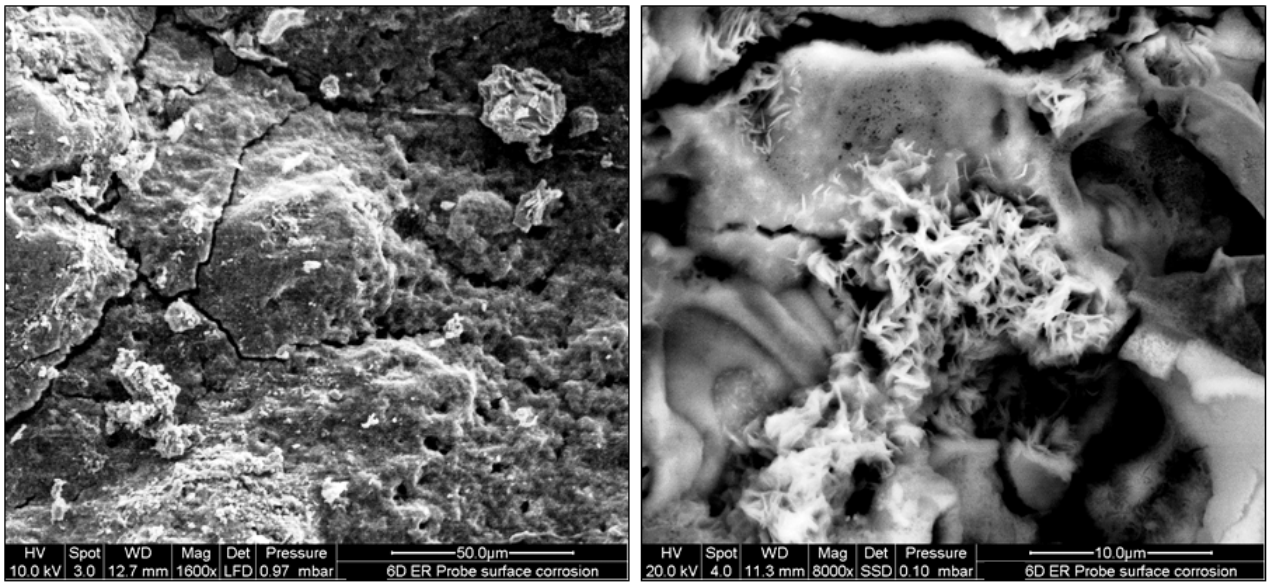

Figure 11 Surface micrograph of cylindrical ER probe exposed to X6D fluid. Note the micro-cracks (left) on the surface of the corrosion product. Filament-like crystals are growing from the iron oxide mass seen at higher magnification (right).

method of manufacturing from which the material is produced (e.g., pipe, bar, forging, casting, plate) rather it provides the chemical composition of the alloy (Baboian, 2005).

From the database, it is noted that the most tested metals are the carbon steels conforming to American Petroleum Institute (API) Specification 5CT or International Standards Organization (ISO) 11960:2004. This standard specifies the steel pipes for use as well casing or tubular for oil and gas

and similarly adopted for geothermal applications. Understandably K55, J55, N80 and L80 carbon steels are well represented in majority of the tests. Also included with this group are the American Iron and Steel Institute (AISI) plain carbon steels 1010, 1018 and 1020 which is compliant with ASTM A519 standard for carbon and alloy steel mechanical tubing. Weathering steel ASTM grades A 588 (COR-TEN® B), grey cast iron, P110 and P235GH (European Standard equivalent to ASTM A106 Grade A carbon steel) has been likewise tested in acid geothermal fluid condition.

Kurata, et al. (1995) use Japanese made chromium-molybdenum (Cr-Mo) steels STBA23, STBA24, STBA25 and STBA 26 that conforms to Japan standard (JIS G3462) for most of their tests. The equivalent ASTM standard for these alloys is A213 or 10216-2 for the European Standard (EN).

Also thoroughly tested in acidic geothermal fluid are the austenitic stainless steel Types 304, 316 and 316L. These are the most popular of the stainless steels because of their ductility, ease of working and good corrosion resistance. These alloys are also not subject to 885ºF (475ºC) embrittlement and to hydrogen embrittlement. However, these are known to be susceptible to chloride stress corrosion cracking. Also within the austenitic group tested in acid geothermal fluid in this database are AL6XN, 904L, 1925hMo, 310, Sanicro 28 (high-alloy austenitic) and 317LM.

Ferritic stainless steels are resistant to chloride stress corrosion cracking, and have high strength and are highly resistant to vibration. Those tested in acidic geothermal fluid in this summary are 405, 430, 444 and E-Brite. This type of steel is known to be subject to 885ºF (475ºC) embrittlement at temperatures as low as 600ºF (315ºC) and susceptible to hydrogen embrittlement. Martensitic stainless steels tested include 410 and 422. Martensitic stainless steels are not highly corrosion resistant and only as good as Type 304. However, these stainless steels have excellent hardness from the carbon added to the alloy. Their ability to maintain a keen edge comes from their high hardness and corrosion resistance. Although SUS630 (equivalent to 17-4PH), is a martensitic stainless steel, it is classified in the precipitation hardening stainless steels category. SUS630 is an ideal metal to use when high strength and corrosion resistance is required.

Alloys 22015, 2507 and SUS329J2L belong to the duplex, types of stainless steel. Duplex stainless steels are characterized by having both austenite and ferrite in their microstructure. Duplex stainless steels are susceptible to 885ºF (475ºC) embrittlement at temperatures as low as 600ºF (315ºC) and to hydrogen embrittlement. The latter is resistant to chloride stress corrosion cracking.

Nickel-based alloys were also substantially tested in acid geothermal fluid. The following are included in the summary: Monel 400, C-276, 625, 825, Alloy 59, Inconel 600, Alloy 20 (Carpenter 20Cb3), Alloy 31, G3. Nickel based alloys are very resistant to corrosion in alkaline environments, neutral chemicals and many natural environments. In addition, many nickel based alloys show excellent resistance to pitting, crevice corrosion and stress corrosion cracking in chloride environments. These alloys however are more expensive than stainless steels (Sorell, 1998) due to high nickel content.

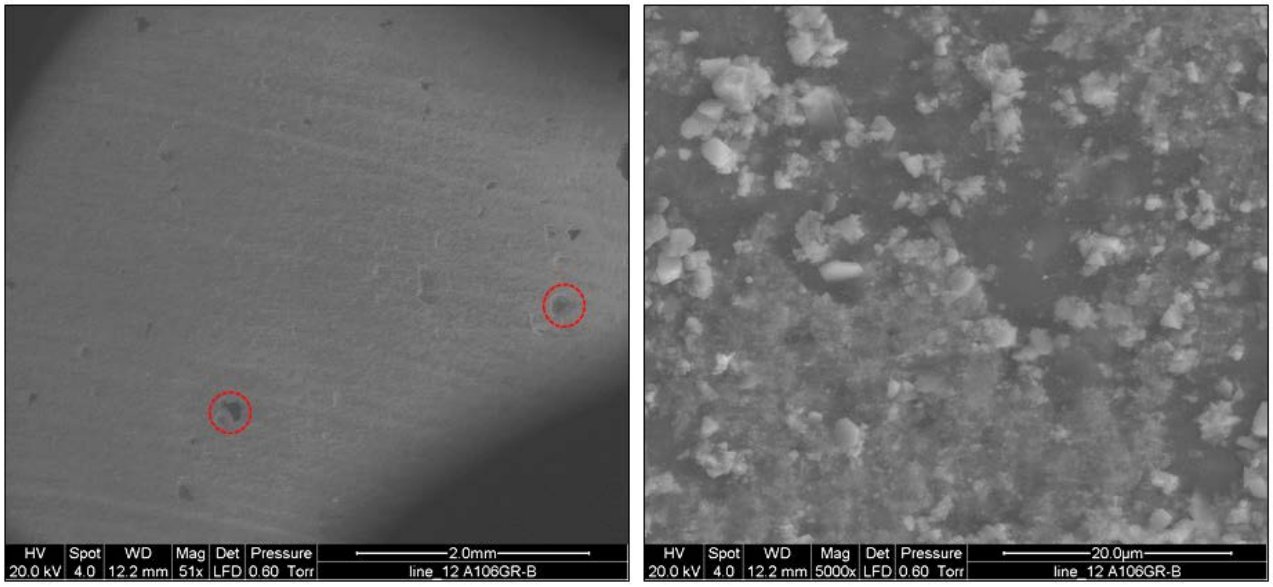

Figure 12 Minute craters (red circles) form on the surface of the corrosion coupon (left). These eventually grow in size and become large crevices seen in Figure 5. Iron oxide crystal formed at the surface of the coupon is seen at higher magnification.

Table 2 Results of analyses of the metal samples surface composition using energy dispersive x-ray analysis (EDS).

	A	B	C	D	E
Element	Composition (in % wt)				
C			6.27	4.34	6.54
O	30.41	26.57	46.43	16.94	18.67
Si	0.52	0.1			19.26
S	1.55	0.22			8.51
Cl	0.19	1.75	0.76	1	
Fe	67.33	71.36	46.53	77.71	19.68
Al					0.52
Zn					12.83
As					13.99
Total	100	100	100	100	100

Another group that is thoroughly tested in acidic geothermal brine is the titanium and titanium alloys (Thomas, 2003). In the database, the following alloys have been tested in addition to pure titanium: Ti-6Al-4V, Titanium Grade 1 and Titanium Grade 2. Other pure metals tested are niobium, nickel, molybdenum and some specialty aluminum (Aluminum 5083) and cobalt (S 816, Haynes 25) alloys.

Corrosion rates were measured using mass-loss coupon exposure method, linear polarization resistance (LPR) technique and potentiodynamic polarization (mainly for localized corrosion such as pitting and crevice corrosion). By far, the most prevalent and the method used to calibrate other measurements are through mass-loss coupon. The authors used different units to measure corrosion rate and no attempt was made in the database to reckon the values to one standard unit. Conversions of the units are straightforward except when using mdd units where density data need to be available to do conversion to mils/y or µm/y. Acceptable corrosion rates for metals in geothermal well environment is <0.l mm/y (Kurata, et al, 1995). Note that the conditions during the tests vary from each experiment especially in terms of fluid velocity. Some tests were done at static or low flow (mainly in laboratory autoclave tests), while others were conducted on the field, such as discharging wells, pipeline by-pass, geothermal test facilities and even in volcanic craters. Corrosion rates measured at static conditions are generally lower than that measured at flows > 100 m/s at pH ≤ 3.2 (Sanada, et al., 1998). Turbulence of the fluid flow also increases the corrosion rates of the test alloys at lower pH and higher temperature. Metals that corroded or have marginally acceptable corrosion rates at static condition in a given geothermal fluid temperature and pH level are expected to have higher corrosion rates at higher fluid velocities.

The mild carbon steels (including API Spec 5CT materials) are not suitable for acidic geothermal fluids with corrosion rates exceeding the threshold value at pH <4.5 (Sanada et al., 1998). Sanada et al (2000) recommends the use of duplex stainless steels for acidic (acid SO_4-Cl) fluids at pH >3 consistent with the data from Kurata, et al, (1992) and Shannon (1977). Schutz and Watkins, (1998) concludes that ruthenium-enhanced titanium alloys "may be the only tubular materials fully resistant enough for development of high-temperature (<330°C), highly acidic (pH<2.3) and sour geothermal brine fields for power generation in the Philippines". From the corrosion data, a number of nickel-based alloys are also potential materials candidates for acidic geothermal fluid.

4. PROPOSED CORROSION TESTS USING CRA'S IN AN ACIDIC GEOTHERMAL ENVIRONMENT

4.1 Field Test Set-Up

Nine (9) types of metals will be tested by exposing sample coupons of each material to flowing acid geothermal fluid in the field. The names (common and UNS) of each metals is shown in Table 3.

The carbon steel coupon (K55) will serve as a normalizing sample from which all other alloys will be compared. K55 is a general purpose pipe material used in geothermal well construction (Sampedro, et al., 1988). Mild alloy steel L80 is also included in the test samples because it is also normally used in wells with expected high concentration of hydrogen sulfide (Ogundele and White, 1987).

The actual chemical composition in weight percent of each alloy as provided by the manufacturers is also shown in the table. Stainless steels 2205 and 2507 are duplex and super-duplex respectively. Classification of standard, super or hyper duplex stainless steels depends on the Pitting Resistance Equivalent Number (PREN). The PREN can be calculated using the equation:

$$PREN = \%Cr + 3.3(\%Mo) + 16(\%N) \quad (5)$$

Standard duplex stainless steels have PREN from 30-40, super-duplex > 40, and hyper-duplex >47. PREN values of 2205 and 2507 are 36 and 42 respectively. A PREN of 32 is considered the minimum for the prevention of seawater pitting resistance. Both alloys have been tested in acidic geothermal environment (Kurata, et al, 1995, Lichti et al, 2010, Sanada, et al, 2000, and Kurata, et a., 1992) and gave acceptable (<0.01 mm/y) corrosion rates. Duplex stainless steels are recommended for use as well casing material by Sanada, et al (2000) for acid sulphate geothermal fluids with pH>3.0.

AL6XN alloy is a super-austenitic stainless steel developed by Allegheny Ludlum Corporation (Malik, et al., 2000). This metal has been tested in RRGE-1 well in Raft River by Miller (1977) and in Magmamax-1 geothermal tests facility in Salton Sea (Carter and McCawley, 1982). Although austenitic stainless steels do not perform well in chloride solutions due to pitting corrosion, the measured general corrosion rate of 6X is < 5 µm/y (Carter and MacCawley, 1982). These tests were carried out at high temperature and in hyper-saline condition. However, this alloy has not been tested yet in pH < 5.2 and maybe worthwhile to test in the low pH range, especially the improved AL6XN type.

Alloys I625, I825, Alloy 59 and Alloy 31 are nickel-based alloys with varying nickel and molybdenum content (Sorell, 1997). These alloys have been substantially tested in high temperature, high salinity and low-pH conditions. Normally, higher nickel and molybdenum content provide better corrosion resistance. Kurata, et al., (1995) concluded that for geothermal fluid at temperature of 300°C and pH 3.0, the suitable material for well construction should have more than 30% (weight) of Cr equivalent and corresponds to duplex stainless steel or an equivalent high Ni - based alloy. Alloy 59 is suitable and represents a safe option to be used in geothermal facilities working with highly saline fluids up to 150 °C (Mundhenk et al., 2013).

Cost is also a consideration in selecting the coupons used in the test. Table 7 shows the cost per equivalent volume of the metals recalculated relative to the cost of K55 casing material. There is economic incentive in testing multiple alloys because the price of each alloy varies to large degree for each type. The cost of alloys also varies with the prevailing price of component metals such as nickel and molybdenum in the market. Ultimately, the application of any of the metals in well or pipeline construction will be influenced by their ability to survive the corrosive acidic geothermal environment as well as those having least cost. Depending on the corrosion rates from the tests and the envisioned maintenance cycle for a component, say a geothermal well, one alloy might become more advantageous economically to another alloy despite higher material cost. This was explained by Love, et al., (1988) in the decision to use Beta-C titanium for highly corrosive wells in the Salton Sea over other alloys with acceptable rates of corrosion.

Coupons used for the test are 1/8" thickness × 3/4" wide × 2" long, with a 3/8" diameter hole in the center and with square corners (± .031") tolerances. Note that 5923HMO coupon is only 1/16" thick. The coupons were polished with 120 grit SIC abrasive. The coupon samples will be mounted onto a titanium grade 2 tests rack (Figure 13). The bolts, nuts and washer holding the coupons are also made from titanium grade 2 alloys to prevent the latter from galvanic corrosion susceptibility. Corrosion can possibly cause the bolts to "snap-off" and can result in coupons being washed away after prolonged exposure to the acidic fluid. The coupons are individually shielded from galvanic corrosion by insertion of Teflon spacers and shoulder washers in between the coupons to prevent metal-to-metal contact. The spacers will also act as artificial crevice spots for the metals to evaluate crevice corrosion after the test.

The rack with the coupons is exposed to the acidic geothermal fluid through the test vessel shown in Figure 13. The vessel is made from 10-inch schedule-40 flanged spool about 1 meter long. Fluid goes into the vessel through a 1-inch carbon steel pipe system tapped from the two-phase branch line of an acidic geothermal well. Fluid exits from the vessel through another 1-inch pipe system that discharges to a mini-silencer. Both vessel pressure and temperature are monitored through two 1 inch ports with attached pressure gauge and thermocouple (Figure 13). The vessel pressure of the vessel during the test is 148 psi (g) and temperature of 172°C. The flow is maintained at 6.3 L/min. Coupon exposure to the acidic fluid is set at 1 month. The pH of the fluid was measured daily to monitor any changes. Chemical analyses of the fluid were carried out weekly. After one month, the rack was retrieved and the coupons disassembled. The coupons were dried in an oven for 1 hour at 60°C and packed in individual Ziploc bags for evaluation.

4.2 Evaluation of Results

The corrosion coupons are currently being evaluated for corrosion rates through weight loss method and surface evaluation using Scanning Electron Microscopy (SEM) coupled with EDS.

Coupons retrieved from the test vessel were oven dried and weighed until constant weights are obtained using an analytical balance with an accuracy of ±0.0001 g. This will be reflected as weight after exposure. An increase in weight may be expected due to scaling or formation of corrosion products. After the weights are determined, the surface condition of the coupons will be evaluated using an FEI Quanta 200F Scanning Electron Microscope with Field Emission Gun (FEG). Any surface defects due to localized corrosion can be observed starting at microscopic (~50×) down to 20,000× magnification. Scale deposits or corrosion products formed on the surface can be compositionally characterized using the energy dispersive x-ray spectroscopy (EDS) analysis. After the surface analyses are completed, the samples will be washed using 9 wt.% hydrochloric acid containing 3.5 g/L inhibitor hexamethylenetetramine, as specified in ASTM Standard G1 (ASTM G1-90, 1999). After all scales and corrosion products are removed, the coupons will be weighed to constant weight using an analytical balance. The resulting coupon weights will be used to calculate the corrosion rate using the equation (Baboian, 2005):

$$Corrosion\ rate = \frac{(K \times W)}{(A \times T \times D)} \quad (5)$$

Where:

K = constant (µm/y)

T = time of exposure in hours to the nearest 0.01 hours

Table 3. Chemical composition of metals and alloys (in weight percent) used for testing as provided by the manufacturers.

		Chemical Composition (% Wt)															
MATERIAL	UNS	C	Si	Mn	P	S	Cu	Cr	Ni	Mo	Al	N	Sr	Ti	Co	Nb	Fe
AL6XN	N08367	0.02	0.4	0.65	0.023	0.0002	0.27	20.62	23.66	6.11		0.24					48.0
I625	N06625	0.02	0.18	0.14	0.008	0.001		22.6	59.68	8.9	0.18			0.25	0.13	3.5	4.4
I825	N08825	0.01	0.2	0.5		0.0004	2	22.2	39	3.3	0.2		0.2	0.9			31.4
2205	S31803	0.014	0.39	1.36	0.022	0.001		22.5	5.7	3.2		0.19					66.6
2507	S32750	0.021	0.18	0.59	0.023	0	0.2	25.6	6.84	3.81		0.29					62.4
5923HMO	N06059	0.004	0.03	0.17	0.002	0.002	0.02	22.55	60.15	15.45	0.31				0.02		1.0
3127HMO	N08031	0.006	0.04	1.6	0.013	0.002	1.22	26.8	31.34	6.5		0.2					31.9
L80		0.25	0.28	0.78	0.011	0.003	0.01	0.98	0.03	0.29	0.4						
K55																	

Table 4. Cost of alloys relative to K55 casing material per unit volume. These costs are for comparison only. Total cost for casing, pipe or other equipment should take into consideration other factors such as length, thickness and connections which have to be sourced directly from suppliers. Cost data were re-calculated from Mundhenk, et al (2012) and from www.EngineeringToolBox.com.

COUPON	TYPE	COST RATIO
AL6XN	superaustenitic stainless steel	13.68
Alloy 625	nickel chromium-molybdenum alloy	31.00
Alloy 825	nickel-chromium alloy with molybdenum + copper	16.52
2205	ferritic-austenitic duplex stainless steel	4.80
2507	super duplex stainless steel	7.84
5923HMO	nickel-chromium-molybdenum alloy	34.32
3127HMO	iron-nickel-chromium-molybdenum alloy + nitrogen	17.08
L80	carbon steel (high strength)	1.00
K55	carbon steel (medium strength)	1.00
Titanium Grade 2	commercially pure titanium	31.32

A = area in cm^2 to the nearest 0.01 cm^2.

W = mass loss in g. to nearest 1 mg (corrected for any loss during cleaning.

D = density of the metal in g/cm^3.

The surface of the clean coupons will be examined through a high-resolution microscope to look for pitting and other surface imperfections due to corrosion.

5. CONCLUSION

Excessive corrosion of carbon steel material used in well casing and tubular and transmission pipelines due to acidic geothermal fluid has been reported by a number of authors. Carbon steel pipe and casing materials are vulnerable to acidic geothermal fluid causing rapid corrosion and failure in a short time.

Carbon steel materials exposed to two highly acidic wells with pH < 3 in the Philippines were evaluated for corrosion damage. Visual evaluation at low magnification showed several material defects in the form of large pits, crevices and visible material loss due to corrosion. There is general corrosion observed throughout the surface of the metal further supporting the corrosion rates measured from the ER probes and corrosion coupon. Analyses of scale composition shows complete transformation of carbon steel metal to iron oxides and oxy-hydroxides with only trace amounts of sulphur, silica and chloride. These trace elements possibly exist as iron compounds as well. Further work is needed to identify each corrosion product formed through their crystal structure using x-ray diffraction or transmission electron microscopy.

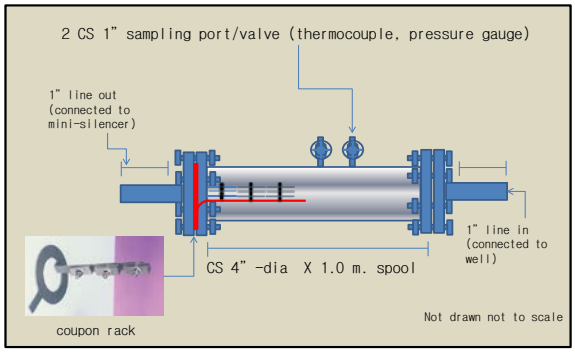

Figure 13 Corrosion test vessel schematic showing the position of the corrosion rack which is held in place by a rack collar sandwiched between the pipe flanges.

The review of corrosion-resistant alloys used in tests on acidic geothermal fluids yielded 87 types of metals and alloys. Titanium, nickel alloys, a few super-austenitic and some duplex stainless steels showed good resistance to acid geothermal fluid with corrosion rates below the acceptable threshold.

Seven potential corrosion resistant alloys and two standard carbon steels (K55 and L80) were field tested in an acid well in the Philippines to determine corrosion behaviour at low velocity condition. The methods for evaluating the results of the field tests include uniform corrosion rate determination through mass-loss method and surface analyses using scanning electron microscopy (SEM) and elemental characterization through energy dispersive spectroscopy (EDS). Alloys that perform well under this condition will be further tested for future well or pipe line application.

6. REFERENCES

Abe, M (1993) Long term use of acidic reservoir at Onikobe Geothermal Power Plant, in Proc. of The 15th New Zealand Geothermal Workshop, pp 5 to 10

Amend, B. and Yee, J. (2013). Selective Application of Corrosion Resistant Alloys Mitigates Corrosion in pH-Modified Geothermal Fluids. Corrosion Conference and Expo. Paper No. 2416

API Specification 5CT (2005) Specification for Casing and Tubing. Eighth Edition, ISO 11960:2004, Petroleum and natural gas industries—Steel pipes for use as casing or tubing for wells

Ármannsson, H., Fridriksson, T., Gudfinnsson, G. H., Ólafsson, M., Óskarsson, F., & Thorbjörnsson, D. (2014). IDDP—The chemistry of the IDDP-01 well fluids in relation to the geochemistry of the krafla geothermal system. *Geothermics*, *49*(0), 66-75.

Arnórsson, S., Stefánsson, A., & Bjarnason, J. Ö. (2007). Fluid-fluid interactions in geothermal systems. *Reviews in Mineralogy and Geochemistry*, *65*(1), 259-312.

ASTM G1-90 (1999). Standard Practice for Preparing, Cleaning, and Evaluation of Corrosion Test Specimens.

Baboian, R. (Ed.). (2005). Corrosion tests and standards: application and interpretation (Vol. 20). ASTM international.

Banning, L. H., & Oden, L. L. (1973). *Corrosion Resistance of Metals in Hot Brines: A Literature Review*,

Borshevska, M., Lichti, K., & Wilson, P. (1982). The relationship between corrosion products and corrosion rates in geothermal steam. *Proceedings of the Pacific Geothermal Conference... Incorporating the... New Zealand Geothermal Workshop*, 191.

Braithwaite, W., & Lichti, K. (1980). Surface corrosion of metals in geothermal fluids at broadlands, new zealand. *Geothermal Scaling and Corrosion*, *ASTM STP*, *717*, 81-112.

Carter, J., & McCawley, F. (1982). Corrosion tests in brine and steam from the salton sea KGRA. *Journal of Materials for Energy Systems*, *3*(4), 30-38.

Casper, L. A., and Pinchback, T. R. (1980). *Geothermal scaling and corrosion : Symposia presented at new orleans, la., 19-20 feb. 1979, and honolulu, hawaii, 4-5 april 1979 / L.A. casper and T.R. pinchback, editors* Philadephia, Pa. 1916 Race St., Philadelphia 19103 : American Society for Testing and Materials c1980.

Chen, C. H. (1970). Geology and geothermal power potential of the tatun volcanic region. *Geothermics*, *2*, *Part 2*(0), 1134-1143.

Cramer, S., & Carter, J. (1980). Corrosion in geothermal brines of the salton sea known geothermal resource area. *ASTM STP*, *717*, 113-141.

Davis, R. B., & M. (1977). Corrosion susceptibilities of various metals and alloys in synthetic geothermal brines. Journal of Materials Science, 12(9), 1909-1913.

F. D'Amore, A.H. Truesdell, J.R. Haizlip (1990). Production of HCl by mineral reactions in high temperature geothermal systems. Proc. 15th Workshop on Geoth. Res. Engng, Stanford, California (1990), pp. 199–210

D'Amore, F., & Bolognesi, L. (1994a). Isotopic evidence for a magmatic contribution to fluids of the geothermal systems of larderello, italy, and the geysers, california. *Geothermics*, *23*(1), 21-32.

D'Amore, F., & Bolognesi, L. (1994b). Isotopic evidence for a magmatic contribution to fluids of the geothermal systems of larderello, italy, and the geysers, california. *Geothermics*, *23*(1), 21-32.

Einarsson, K., Pálsson, B., Gudmundsson, Á., Hólmgeirsson, S., Ingason, K., Matthíasson, J., & Ármannsson, H. (2010). Acid wells in the Krafla geothermal field. In Proceedings of the world geothermal congress (pp. 1-6).

Ellis, P. F., & Conover, M. F. (1981). Materials selection guidelines for geothermal energy utilization systems. *NASA STI/Recon Technical Report N*, *81*, 22566.

Ellis, P. (1985). Companion study guide to short course on geothermal corrosion and mitigation in low temperature geothermal heating systems. *Radian Corporation, Austin, Texas*,

Gherardi, F., Panichi, C., Yock, A., & Gerardo-Abaya, J. (2002). Geochemistry of the surface and deep fluids of the Miravalles volcano geothermal system (Costa Rica). Geothermics, 31(1), 91-128.

GOLDBERG, A., & OWEN, L. B. (1979). Pitting corrosion and scaling of carbon steels in geothermal brine. *Corrosion*, *35*(3), 114-124.

Harrar, J. E., McCright, R., & Goldberg, A. (1977). Field electrochemical measurements of corrosion characteristics of materials in hypersaline geothermal brine. *NASA STI/Recon Technical Report N*, *78*, 28656.

Harrar, J. E., Fischer, J. W., Beiriger, W. J., Steele, W. J., Digiallonardo, S. A., & McCoy, D. D. (1979). Incipient processes in the corrosion of mild steel in 90°C hypersaline geothermal brine. *Corrosion Science*, *19*(7), 819-833.

Harrar, J. E., McCright, R. D., & Goldberg, A. (1978). CORROSION CHARACTERISTICS OF MATERIALS IN HYPERSALINE GEOTHERMAL BRINE. *SAMPE Q*, *10*(1), 1-15.

Hirtz, P., C. Buck, C. and R. Kunzmann (1991). Current techniques in acid chloride corrosion control and monitoring at the Geysers. Proceedings of Sixteenth Workshop on Geothermal Reservoir Engineering, Stanford University, Stanford, CA, USA (1991), pp. 83–95

Holligan, D., Cron, C., Love, W., & Buster, J. (1989). Performance of beta titanium in a salton sea field geothermal production well. *SPE/IADC Drilling Conference*,

Kain, V. (2012). *Corrosion-resistant materials-12* Elsevier Inc. doi:10.1016/B978-0-12-385142-0.00012-X

Keserovic, A., & Bäßler, R. (2013). *Material evaluation for application in geothermal systems in indonesia*

Kiyosu, Y., & Kurahashi, M. (1983). Origin of sulfur species in acid sulfate-chloride thermal waters, northeastern Japan. Geochimica et Cosmochimica Acta, 47(7), 1237-1245.

Koestono, H. (2010) Lahendong Geothermal Field, Indonesia: Geothermal Model Based on Wells LHD-23 and LHD-28. Report No. 3, UNU Geothermal Training Programme.

Kritzer, P. (2004). Corrosion in high-temperature and supercritical water and aqueous solutions: A review. *The Journal of Supercritical Fluids*, *29*(1–2), 1-29.

Karlsdottir, S. N., Ragnarsdottir, K. R., Moller, A., Thorbjornsson, I. O., & Einarsson, A. (2014). On-site erosion–corrosion testing in superheated geothermal steam. Geothermics, 51(0), 170-181.

Kurata, Y., Sanada, N.,Nanjo, H., Ikeuchi, J. (1992). Material damages in geothermal power plants. *Proceedings 14th New Zealand Geothermal Workshop*, *1*(1), 159-164.

Kurata, Y., Sanada, N., Nanjo, H. and Ikeuchi, J. (1995) CASING PIPE MATERIALS FOR DEEP GEOTHERMAL WELLS. Geothermal Resources Council TRANSACTIONS, Vol. 19, pp 105 -109

Lichti, K.A., Engelberg, D.,Young, M.G. (1999). Corrosion in simulated acidic geothermal well fluids. 21st New Zealand Geothermal Workshop, 1(1), 187-192.

Lichti, KA, Julian, R.H,. (2010). Corrosion and scaling in high gas (25%) geothermal fluids. *Proceedings World Geothermal Congress 2010*, , 1-8.

Lichti, K., White, S., Ko, M., Villa Jr, R., Siega, F., Olivar, M., Buning, B. (2010). Acid well utilisation study: Well MG-9D, philippines. *Proceedings World Geothermal Congress, Bali, Indonesia*, 25-29.

Malik, A. U., Prakash, T.L., Ahmed, S., Andijani, I. N., Al-Muaili, F. and John O'Hara (2000) CORROSION PERFORMANCE EVALUATION OF ALLOY AL-6XN®1. Issued as Technical Report No.R. 3804/EVP 95018.

Marini, L., Yock Fung, A., & Sanchez, E. (2003). Use of reaction path modeling to identify the processes governing the generation of neutral Na–Cl and acidic Na–Cl– SO4 deep geothermal liquids at Miravalles geothermal system, Costa Rica. Journal of volcanology and geothermal research, 128(4), 363-387.

Marshall, T.; Hugil, A. J. (1957). Corrosion by low pressure geothermal steam. Corrosion, 13, 329t.

Marshall, T., Braithwaite, W.R. (1973). A review of "GEOTHERMAL ENERGY" review of research and development christopher H. armstead, UNESCO, editor united nations educational, scientific and cultural organization, paris, 1973.186 pages.£ 14.00. *Corrosion Control in Geothermal Systems*, *1*(1), 151-160.

Matsuda, K., Shimada, K., & Kiyota, Y. (2005). ISOTOPE TECHNIQUES FOR CLARIFYING ORIGIN OF SO4 TYPE ACID GEOTHERMAL-FLUID—CASE STUDIES OF GEOTHERMAL AREAS IN KYUSHU, JAPAN. *Use of Isotope Techniques to Trace the Origin of Acidic Fluids in Geothermal Systems.IAEA-TECDOC-1448*, , 83-95.

McCawley, F. X., Cramer, S., Riley, W., Carter, J., & Needham Jr, P. (1981). *Corrosion of Materials and Scaling in Low-Salinity East Mesa Geothermal Brines,*

Miller, R. (1980). Chemistry and materials in geothermal systems. *Geothermal Scaling and Corrosion: Symposia Presented at New Orleans, La., 19-20 Feb. 1979, and Honolulu, Hawaii, 4-5 April 1979,* (717) 1.

Miranda-Herrera, C., Sauceda, I., González-Sánchez, J., & Acuña, N. (2010). Corrosion degradation of pipeline carbon steels subjected to geothermal plant conditions. *Anti - Corrosion Methods and Materials, 57*(4), 167-172.

Mundhenk, N., Huttenloch, P., Kohl, T., Steger, H., & Zorn, R. (2013). Metal corrosion in geothermal brine environments of the upper rhine graben – laboratory and on-site studies. *Geothermics, 46*(0), 14-21.

Mundhenk, N., Huttenloch, P., Sanjuan, B., Kohl, T., Steger, H., & Zorn, R. (2013). Corrosion and scaling as interrelated phenomena in an operating geothermal power plant. *Corrosion Science, 70*(0), 17-28.

Needham Jr, P. B., Riley, W. D., Conner, G. R., & Murphy, A. P. (1980). Chemical Analyses of Brines From Four Imperial Valley CA Geothermal Wells. Society of Petroleum Engineers Journal, 20(02), 105-112.

Noguchi, K., Goto, T., Ueno, S., & Imahashi, M. (1970). A geochemical investigation of the strong acid water from the bored wells in hakone, japan. *Geothermics, 2, Part 1*(0), 561-563.

NZS 2403:1991, (1991). NZ Code of Practice for Deep Geothermal Well

Ogundele, G., & White, W. (1987). Observations on the influences of dissolved hydrocarbon gases and variable water chemistries on corrosion of an API-L80 steel. *Corrosion, 43*(11), 665-673.

Z. Pang, Z. (2005). Summary of the Co-coordinated research project. IAEA, Use of Isotope Techniques to Trace the Origin of Acidic Fluids in Geothermal Systems, IAEA TECDOC-1448 (2005) ISSN 1011-4289

Pang, Z. (2006). pH dependant isotope variations in arc-type geothermal waters: New insights into their origins. *Journal of Geochemical Exploration, 89*(1–3), 306-308.

Posey, F., & Palko, A. (1979). Corrosivity of carbon steel in concentrated chloride solution. *Corrosion, 35*(1), 38-43.

Reyes, A. G. (1985). A comparative study of 'acid' and neutral-pH' hydrothermal alteration in the Bacon-Manito Geothermal Area, Philippines. MS Thesis. University of Auckland, NZ.

Reyes, A. G., & Cardile, C. M. (1989). Characterization of clay scales forming in philippine geothermal wells. *Geothermics, 18*(3), 429-446.

Reyes, A. G., Giggenbach, W. F., Saleras, J. R. M., Salonga, N. D., & Vergara, M. C. (1993). Petrology and geochemistry of alto peak, a vapor-cored hydrothermal system, leyte province, philippines. *Geothermics, 22*(5–6), 479-519.

Salonga, N. D., Bayon, F. E. B., & Martinez, M. (2000). The implication of 34S and I8O isotope systematics on the sulfur cycle in mahanagdong hydrothermal system (philippines). *Proceedings of the World Geothermal Congress 2000,* 2845-2850.

Sampedro, J. A., Rosas, N., Díaz, R., & Domínguez, B. (1988). Developments in geothermal energy in mexico—part nineteen. corrosion in mexican geothermal wells. *Heat Recovery Systems and CHP, 8*(4), 355-362.

Sanada, N., Kurata, Y., Nanjo, H., Kim, H., Ikeuchi, J., & Lichti, K. A. (2000). IEA deep geothermal resources subtask C: Materials, progress with a database for materials performance in deep and acidic geothermal wells. *Proceedings of World Geothermal Congress, International Geothermal Association (IGA), May,* 2411-2416.

Sanada, N., & Lichti, K. (1997). Prospects for the evaluation and development of materials under IEA research collaboration program on deep geothermal resources. *Proc NEDO Int'l Geothermal Symposium, Japan,* 192-199.

Sanada, N., Kurata, Y., & Lichti, K. A. (1997). Valuation and development of deep geothermal resources - materials subtask update of IEA research collaboration program. *Transactions - Geothermal Resources Council, , 21* 317-324.

Schutz, R., & Watkins, H. (1998). Recent developments in titanium alloy application in the energy industry. *Materials Science and Engineering: A, 243*(1), 305-315.

Shannon, D. (1977). *CORROSION OF IRON-BASE ALLOYS VERSUS ALTERNATE MATERIALS IN GEOTHERMAL BRINES (Interim Report-Period Ending October 1977),Batelle -Pacific Northwest Laboratories*

Shannon, D., Morrey, J., & Smith, R. (1977). Use of a chemical equilibrium computer code to analyze scale formation and corrosion in geothermal brines. *SPE International Oilfield and Geothermal Chemistry Symposium,*

Shindo, D. and T. Oikawa (2002), Analytical Electron Microscopy for Materials Science. Springer, Tokyo.

Shreir, L. L. (1976). *Corrosion. vol. I. metal/environment reactions.* Butterworth & Co.(Publishers) Ltd.

Sorell, G., (1998). Corrosion- and heat-resistant nickel alloys guideline for selection and application. Nickel Development Institute.

Sugiaman, F., Sunio, E., Molling, P., & Stimac, J. (2004). Geochemical response to production of the tiwi geothermal field, philippines. *Geothermics, 33*(1–2), 57-86.

Tello, E., Verma, M. P., & Tovar, R. (2000). Origin of acidity in the los humeros, mexico, geothermal reservoir. *Proceedings World Geothermal Congress, Kyushu-Tohoku, Japan,* 2161-2167.

Thomas, R. (2003). Titanium in the geothermal industry. *Geothermics, 32*(4–6), 679-687.

Tolivia, M. E. (1970). Corrosion measurements in a geothermal environment. Geothermics, 2, Part 2(0), 1596-1601.

Truesdell, A. H. (1992) ORIGINS OF ACID FLUIDS IN GEOTHERMAL RESERVOIRS. Geothermal investigations

with isotope and geochemical techniques in Latin America IAEA-TECDOC-641

Truesdell, A., & Nakanishi, S. (2005). Chemistry of neutral and acid production fluids from the onikobe geothermal field, miyagi prefecture, honshu, japan. *Use of Isotope Techniques to Trace the Origin of Acidic Fluids in Geothermal Systems, 1448*, 169.

Truesdell, A. H., Haizlip, J. R., Armannsson, H., & D'Amore, F. (1989). Origin and transport of chloride in superheated geothermal steam. *Geothermics, 18*(1–2), 295-304.

Ueda, A., Kubota, Y., Katoh, H., Hatakeyama, K., & Matsubaya, O. (1991). Geochemical characteristics of the Sumikawa geothermal system, northeast Japan. Geochemical journal, 25(4), 223-244.

Villa, R.R., (2000): A Demonstration of the Feasibility of Acid Well Utilization: The Philippines' Well MG9D Experience, Proceedings, 21st Annual PNOC-EDC Geothermal Conference, (2000), 25–32.

Walters, M.A., Sternfeld, J.F., Haizlip, J.R., Drenick, A.F., and Combs, J.B. (1988). "A Vapor-Dominated Reservoir Exceeding 600'F at The Geysers, Sonoma County, California," Proceedings, Stanford Geothermal Reservoir Engineering Workshop.

White, D. E. and A.H. Truesdell (1969). Geothermal resources of Taiwan - An evaluation of existing data, U.N. Report.

Zarrouk, S. J. (2004) EXTERNAL CASING CORROSION IN NEW ZEALAND'S GEOTHERMAL FIELDS, *Proceedings 26th New Zealand Geothermal Workshop*

ACKNOWLEDGEMENTS

I wish to thank my colleagues at Energy Development Corporation (EDC), especially from Leyte Geothermal Business Unit (LGBU) who provided assistance for the field tests. Gratitude is also extended to Catherine Hobbis, Steve Strover and Dr. Alec Asadov of Research Centre for Surface and Materials Science at University of Auckland Faculty of Engineering for their guidance in the laboratory work.